MIRROR-CURVES AND KNOT MOSAICS

Slavik Jablan

The Mathematical Institute, Knez Mihailova 36, P.O.Box 367, 11001 Belgrade, Serbia, E-mail: sjablan@gmail.com

Ljiljana Radović

University of Niš, Faculty of Mechanical Engineering, A. Medvedeva 14, 18 000 Niš, Serbia, E-mail: ljradovic@gmail.com

Radmila Sazdanović

Department of Mathematics, University of Pennsylvania, 209 South 33rd Street, Philadelphia, PA 19104-6395, USA, E-mail: radmilas@gmail.com

Ana Zeković

Zeta System, Golsvortijeva 1, 11000 Belgrade, Serbia, E-mail: ana@zeta.rs

Abstract

Inspired by the paper on quantum knots and knot mosaics [23] and grid diagrams (or arc presentations), used extensively in the computations of Heegaard-Floer knot homology [2, 3, 7, 24], we construct the more concise representation of knot mosaics and grid diagrams via mirror-curves. Tame knot theory is equivalent to knot mosaics [23], mirror-curves, and grid diagrams [3, 7, 22, 24]. Hence, we introduce codes for mirror-curves treated as knot or link diagrams placed in rectangular square grids, suitable for software implementation. We provide tables of minimal mirror-curve codes for knots and links obtained from rectangular grids of size 3×3 and $p \times 2$ ($p \leq 4$), and describe an efficient algorithm for computing the Kauffman bracket and L-polynomials [18, 19, 20] directly from mirror-curve representations.

Keywords: Knot, link, mirror-curve, knot mosaic, grid diagram, Kauffman bracket polynomial, L-polynomial.

1. Introduction

Mirror-curves originated from matting, plaiting, and basketry. They appear in arts of different cultures (as Celtic knots, Tamil threshold designs, Sona sand drawings...), as well as in works of Leonardo and Dürer [1, 4, 5, 13, 14, 15, 16, 18]. P. Gerdes recognized their deep connection with the mathematical algorithmic-based structures: knot mosaics, Lunda matrices, self-avoiding curves, and cell-automata [13, 14, 15, 16]. Combinatorial complexity of Sona sand drawings is analyzed by M. Damian *et all* [9] and E.D. Demaine *et all* [10].

Mirror-curves are constructed out of rectangular square grids, denoted by $RG[p, q]$, of dimensions p, q ($p, q \in N$). First we connect the midpoints of adjacent edges of $RG[p, q]$ to obtain a 4-valent graph: every vertex of this graph is incident to four edges, called *steps*. Next, choose

a starting point and traverse the curve so that we leave each vertex via the middle outgoing edge. Returning to the starting point, is equivalent to closing a path called a *component*. If we return to the starting point without traversing all of the steps, we choose a different one and repeat the process until every step is used exactly once. A *mirror-curve* in $RG[p, q]$ grid is the set of all components. To obtain a knot or a link diagram from a mirror-curve we introduce the "over-under" relation, turning each vertex to the crossing, i.e., we choose a pair of collinear steps (out of two) meeting at a vertex to be the overpass [18, 19, 20, 25].

Mirror-curves can also be obtained from the following physical model which, in a way, justifies their name: assume that the sides of our rectangular square grid $RG[p, q]$ are made of mirrors, and that additional internal two-sided mirrors are placed between the square cells, coinciding with an edge, or perpendicular to it in its midpoint. If a ray of light is emitted from one edge-midpoint at an angle of $45°$, it will eventually come back to its starting point, closing a component after series of reflections. If some steps remained untraced, repeat the whole procedure starting from a different point.

Through the rest of the paper the term "mirror-curves" will be used for labeled mirror-curves. Hence, all crossings will be signed, where $+1$ corresponds to the positive, and -1 to negative crossings.

Theorem 1. [15] *The number of components of a knot or link L obtained from a rectangular grid $RG[p, q]$ without internal mirrors is $c(L) = GCD(p, q)$.*

The web-Mathematica computations with mirror-curves are available at the address

`http://math.ict.edu.rs:8080/webMathematica/mirror/cont.htm`

2. Coding of mirror-curves

Mirror-curve is constructed on a rectangular grid $RG[p, q]$ with every internal edge labeled $1, -1, 2$, and -2, where $+1$ and -1 denote, respectively, a positive and negative crossing in the middle point of the edge, see Figure 1a, while 2 and -2 denote a two-sided mirror containing the middle point of an edge, either collinear or perpendicular to it. The code for the mirror-curves can be given in matrix form, containing labels of internal edges corresponding to rows and columns of the $RG[p, q]$. For example, the code

$$Ul = \{\{-2, -1, -1, 2\}, \{1, 2, -1, 1\}, \{2, 1, -1\}, \{1, -2, -1\}, \{1, -2, -1\}\}.$$

corresponds to the mirror-curve on Figure 1c, based on the labeled rectangular grid $RG[3, 2]$ shown in Figure 1b.

Our convention is the natural one: we list labels in the rows from left to right, and in the columns from bottom to the top.

3. Reduction of mirror-curves

Labeled mirror-curves represent knot and link (shortly *KL*) diagrams. In this section we consider Reidemeister moves, expressed in the language of mirror-curves.

The Reidemeister move RI is equivalent to replacing crossing by the mirror -2 (i.e., $\pm 1 \rightarrow -2$), see Figure 2a.
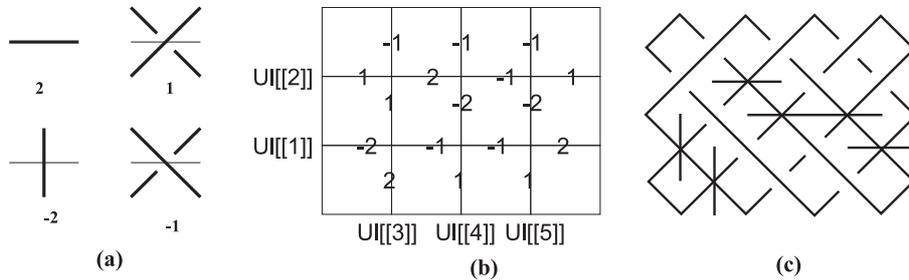
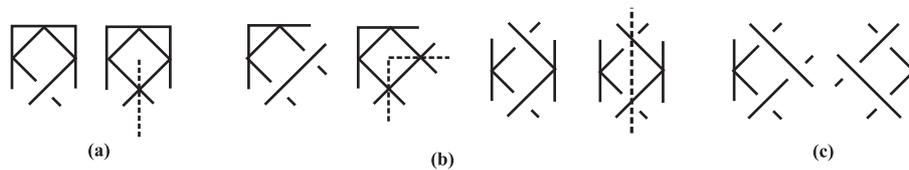Figure 1: (a) Edge labeling; (b) labeled $RG[3,2]$; (c) the mirror-curve corresponding to the code Ul.

Figure 2: (a) Reidemeister move RI; (b) Reidemeister move RII; (c) Reidemeister move RIII, with additional mirrors in RI and RII denoted by dotted lines.

Reidemeister move RII is the replacement of two neighboring crossings of the same sign by two perpendicular or collinear mirrors shown on Figure 2b, and Reidemeister move RIII is illustrated in Figure 2c.

Notice that every unknot or unlink can be reduced to the code containing only labels 2 and -2. For example, the non-minimal diagram of an unknot with three crossings on Figure 3a, given by the code $Ul = \{\{-2,-1\},\{1,1\}\}$, can be reduced using the second Reidemeister move RII applied to the upper right crossings, to $Ul = \{\{-2,-2\},\{1,-2\}\}$ on Figure 3b. This code can be reduced further using the first Reidemeister move RI applied to the remaining crossing, yielding the minimal code of the unknot in $RG[2,2]$: $Ul = \{\{-2,-2\},\{2,-2\}\}$.

Minimal diagrams of mirror-curves correspond to codes with the minimal number of ± 1 labels. Minimal mirror-curve codes of alternating knots and links contain either 1's or -1's, but not both of them.
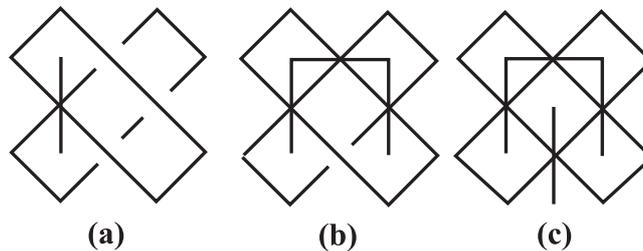

Figure 3: A sequence of Reidemeister moves reducing 3-crossing diagram of an unknot to the minimal one.

Next we consider several examples to illustrate the reduction process. Sometimes it is useful to use topological intuition to simplify the reduction, such as the mirror-moves shown in Figure 4, where the repositioned mirror is shown by a dotted line.
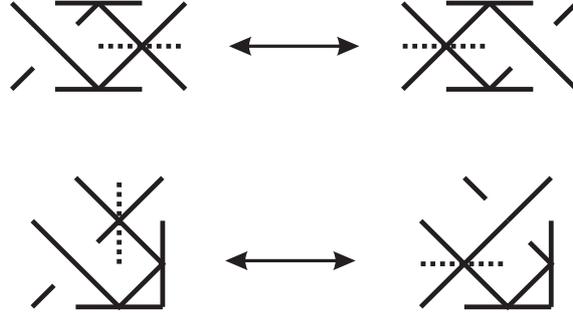
3

Figure 4: Mirror moves that can be useful for simplifying the reduction process.

K. Reidemeister proved that any two different diagrams of the same knot or link are related by a finite sequence of Reidemeister moves, but there are no algorithms prescribing the order in which they can be used. Similarly, we have no algorithms for reducing mirror-curve codes. In particular, we can not guarantee that we can obtain the minimal code without increasing the size of the rectangular grid.

Example 2. *This is the reduction sequence for the 2-component link shown in Figure 5a, determined by the following code*

$$\{\{-2, -1, -1, 2\}, \{1, 2, -1, 1\}, \{2, 1, -1\}, \{1, -2, -1\}, \{1, -2, -1\}\}$$

resulting in the unlink. First we apply the first Reidemeister move RI to the right lower crossing in Figure 5b, and three moves RII, in order to obtain the code

$$\{\{-2, -2, -1, 2\}, \{-2, 2, 2, -2\}, \{2, 1, -2\}, \{-2, -2, -1\}, \{-2, -2, -2\}\},$$

then the mirror-move to the first mirror in the upper row and obtain the code corresponding to the Figure 5c:

$$\{\{-2, -2, -1, 2\}, \{-2, 2, -1, -2\}, \{2, 1, -1\}, \{-2, -2, -2\}, \{-2, -2, -2\}\}.$$

Next we perform two Reidemeister moves RI to obtain Figure 5d, and the code

$$\{\{-2, -2, -1, 2\}, \{-2, 2, 2, -2\}, \{2, 1, -1\}, \{-2, -2, -2\}, \{-2, -2, -2\}\},$$

and the link shown in Figure 5e:

$$\{\{-2, -2, 2, 2\}, \{-2, 2, 2, -2\}, \{2, 1, -1\}, \{-2, -2, -2\}, \{-2, -2, -2\}\}.$$

Finally, the second Reidemeister move RII eliminates the remaining two crossings to obtain the minimal code see Figure 5f,

$$\{\{-2, -2, 2, 2\}, \{-2, 2, 2, -2\}, \{2, 2, 2\}, \{-2, -2, -2\}, \{-2, -2, -2\}\}.$$

Mirror-curve codes can be extended to virtual knots and links, by marking virtual crossings by zeros [21].
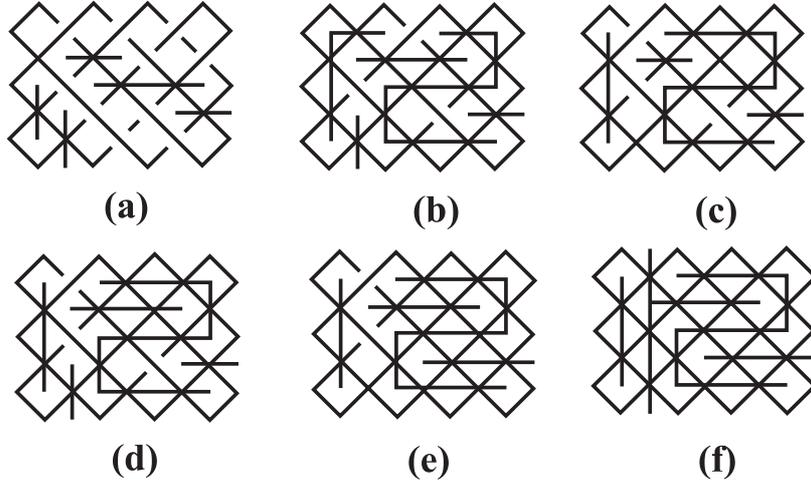
4

Figure 5: Reduction of two-component unlink $Ul = \{\{-2, -1, -1, 2\}, \{1, 2, -1, 1\}, \{2, 1, -1\}, \{1, -2, -1\}, \{1, -2, -1\}\}$.

4. Derivation of knots and links from mirror-curves

Another interesting open problem is which knots and links can be obtained from a rectangular grid $RG[p, q]$ of a fixed size. To remove redundancies, we list each knot or link only once, associated only with the smallest rectangular grid from which it can be obtained.

Obviously, grid $RG[1, 1]$ contains only the unknot, while from $RG[2, 1]$ we can additionally derive the trivial two-component unlink. In general, every rectangular grid $RG[p, 1]$ contains the trivial p-component unlink.

In the rest of the paper, knots and links will be given by their classical notation and Conway symbols [6, 18] from Rolfsen's tables [25]. Links with more than 9 crossings are given by Thistlethwaite's link notation [3].

Grid $RG[2, 2]$ contains the following four knots and links shown in Figure 6: link 4 (4_1^2) given by the code $\{\{1, 1\}, \{1, 1\}\}$, one non-minimal diagram of the Hopf link given by the code $\{\{1, 1\}, \{1, -1\}\}$ which can be reduced to the minimal diagram $\{\{1, -2\}, \{1, -2\}\}$ using the second Reidemeister move RII, the symmetrical minimal diagram of the Hopf link on Figure 6d, given by the code $\{\{-2, -2\}, \{1, 1\}\}$, and the minimal diagram of trefoil (Figure 6e) given by the code $\{\{-2, 1\}, \{1, 1\}\}$.
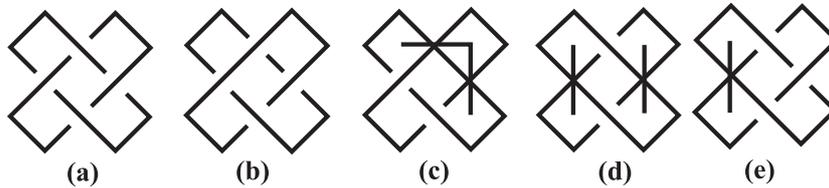

Figure 6: (a) Link 4 (4_1^2); (b) non-minimal diagram of the Hopf link 2 (2_1^2); (c, d) two minimal diagrams of the Hopf link; (e) minimal diagram of the trefoil knot 3 (3_1).

Rectangular grid $RG[2, 2]$ without internal mirrors, taken as the alternating link, corresponds

to the code which contains no ± 2 and all 1's or exclusively -1's. It represents the link 4 (4_1^2) (or its mirror image). Hence, the following two questions are equivalent:

- which *KL*s can be obtained as mirror-curves from $RG[2, 2]$;

- which *KL*s can be obtained by substituting crossings of the link 4 (4_1^2) by elementary tangles 1, -1, L_0 and L_∞, see Figure 6.

In analogy with the state sum model for the Kauffman bracket polynomial [19], where each crossing can be replaced by one of the two smoothings (resolutions) we can consider all possible states of a given rectangular grid $RG[p, q]$, corresponding to four different choices of placing a mirror 2, -2, or one of the crossings 1, -1 at the middle point of each edge. In this light, different mirror-curves obtained in this way can be thought of as all possible states of $RG[2, 2]$, while the corresponding *KL*s can be viewed as all states of the link 4 (4_1^2).
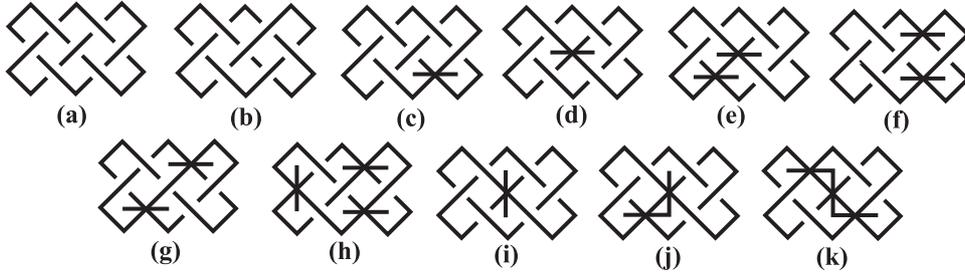

Figure 7: (a) Knot 3 1 3 (7_4); (b) knot 4 2 (6_1); (c) knot 3 1 2 (6_2); (d) link 6 (6_1^2); (e) knot 5 (5_1); (f) knot 3 2 (5_2); (g) Whitehead link 2 1 2 (5_1^2); (h) figure-eight knot 2 2 (4_1); (i) direct product of two trefoils 3#3; (j) direct product of trefoil and Hopf link 3#2; (k) direct product of two Hopf links 2#2.

From $RG[3, 2]$ and its corresponding alternating knot 3 1 3 (7_4) given by the code {{1, 1, 1}, {1, 1}, {1, 1}} on Figure 7a, we obtain knots and links shown on Figure 7b–h:

KL	Mirror-curve code
4 2	{{1, 1, −1}, {1, 1}, {−1, −1}}
3 1 2 (6_2)	{{1, 1, 1}, {1, 1}, {−2, 1}}
6 (6_1^2)	{{1, 2, 1}, {1, 1}, {1, 1}}
5 (5_1)	{{1, 2, 1}, {−2, 1}, {1, 1}}
3 2 (5_2)	{{1, 1, 1}, {1, 1}, {−2, −2}}
2 1 2 (5_1^2)	{{1, 1, 1}, {−2, 1}, {1, −2}}
2 2 (4_1)	{{−2, 1, 1}, {1, 1}, {−2, −2}}

and the following composite knots and links shown on Figure 7i-k: direct product of two trefoils 3#3 given by the code {{1, −2, 1}, {1, 1}, {1, 1}}, direct product of a trefoil and Hopf link 3#2 given by the code {{1, −2, 1}, {−2, 1}, {1, 1}}, and direct product of two Hopf links 2#2 given by the code {{1, −2, 1}, {1, −2}, {−2, 1}}. In the case of composite knots and links we can also obtain their non-alternating versions, e.g., 3#(−3).

Alternating link 3 1 2 1 3 ($L10a_{101}$ from Thistlethwaite's tables) corresponds to $RG[4, 2]$. The following prime knots and links can be obtained from $RG[4, 2]$: 5 1 3 (9_5), 3 1 2 1 2 (9_{20}), 4 1 1 3 (9_5^2), 3 1 3 2 (9_8^2), 3 1 1 1 3 (9_9^2), 5 1 2 (8_2), 4 1 3 (8_4), 3 1 1 1 2 (8_{13}), 8 (8_1^2), 4 2 2 (8_3^2), 3 2 3 (8_4^2),

$3\,1\,2\,2\,(8_5^2)$, $2\,4\,2\,(8_6^2)$, $2\,1\,2\,1\,2\,(8_7^2)$, $7\,(7_1)$, $5\,2\,(7_2)$, $2\,2\,1\,2\,(7_6)$, $2\,1\,1\,1\,2\,(7_7)$, $4\,1\,2\,(7_1^2)$, $3\,1\,1\,2$ (7_2^2), $2\,3\,2\,(7_3^2)$, $2\,1\,1\,2\,(6_3)$, $3\,3\,(6_2^2)$, and $2\,2\,2\,(6_3^2)$.

Moreover, we have a family of rational knots and links corresponding to rectangular grids $RG[p,2]$ ($p \geq 3$), starting with $3\,1\,3\,(7_4)$, $3\,1\,2\,1\,3\,(L10a_{101})$, $3\,1\,2\,1\,2\,1\,3$, ... given by their minimal diagrams $3\,1\,3$, $(((1,(3,1),1),1),1,1,1)$, $((1,(1,(1,(1,(1,3),1)),1)),1,1,1)$, ... Rational knots, also known as 2-bridge knots or 4-plats[1], form the subset of mirror-curves derived from rectangular grids $RG[p,2]$.

Theorem 3. *All rational knots and links can be derived as mirror-curves from rectangular grids $RG[p,2]$ ($p \geq 2$).*
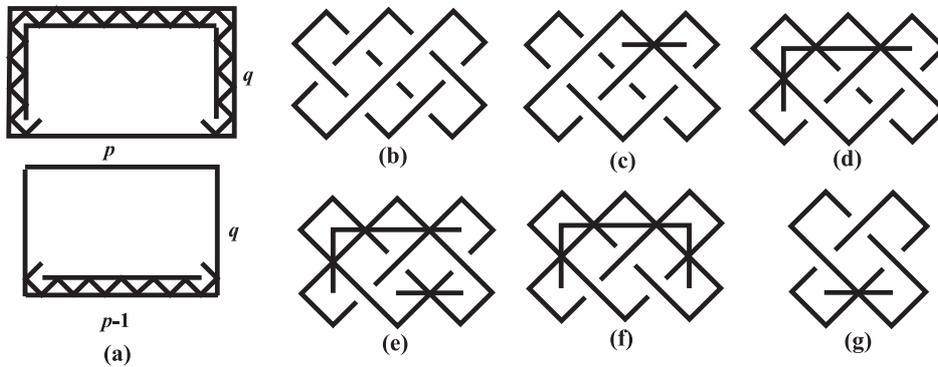

Figure 8: (a) Grid reduction by the all-over move; (b-g) six-step reduction of the knot $3-1\,3$ placed in the $RG[3,2]$ to the trefoil placed in its minimal grid $RG[2,2]$.

The reduction process we have described will not always result in the minimal rectangular grid for representing a given KL as a mirror-curve. Therefore we need a move that reduces the size of the grid, so-called "all-over move", see Figure 8a, reducing the size of the grid from $RG[p,q]$ to $RG[p-1,q]$ while preserving the knot or link type.

The complete reduction of a non-minimal diagram of a trefoil, given by the sequence of codes: $\{\{-1,1,-1\},\{-1,-1\},\{-1,-1\}\} \rightarrow \{\{1,1,-1\},\{1,-1\},\{-1,-2\}\} \rightarrow \{\{-2,1,-1\}, \{1,-2\}, \{-1,-2\}\} \rightarrow \{\{-2,1,-1\},\{1,-2\},\{-2,-2\}\} \rightarrow \{\{-2,1,-2\},\{1,-2\},\{1,-2\}\} \rightarrow \{\{-1,-1\},\{-2,-1\}\}$, including grid reduction from $RG[3,2]$ to $RG[2,2]$ in the last step, is illustrated in Figure 8b-g.

The next natural question is how to construct a mirror-curve representation of a knot or link given in Conway notation [6, 18, 25]. We do not provide the general algorithm, but illustrate the process in the case of figure-eight knot $2\,2$. Knowing that the figure-eight knot is obtained as a product of two tangles 2, Figure 9a, we start by connecting two appropriate ends, see Figure 9b, and proceeding with completing the tangle $2\,2$ and its numerator closure. In this process we are likely to obtain the empty regions, Figure 9e. They can be incorporated in the construction by extending the mirror-curve across the empty region included in our drawing by the Reidemeister move RI. This is achieved by deleting a border mirror and changing the hole into a loop. Most

---

[1]Knots or two component links obtained by a so-called horizontal closure of a braid on 4 strings, with bottom connection points A, B, C, D, and the top connection points A', B', C', D', where we connect A to B, C to D, A' to B', and C' to D'.
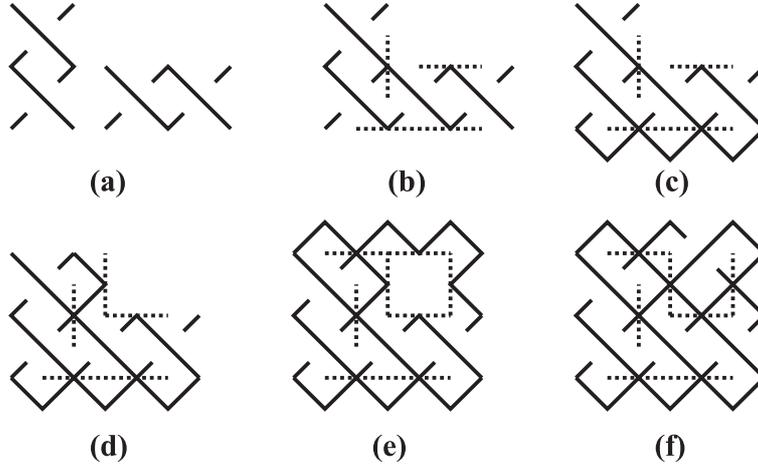
Figure 9: Construction of a mirror-curve diagram of the figure-eight knot 4_1 from its Conway symbol $2\,2$.

often, mirror-curve representation obtained in this way will not be the minimal one in terms of the grid size, so we need to make further reductions[2].

From $RG[3,3]$ and its corresponding alternating 3-component link $8^*2 : 2 : 2 : 2$ with 12 crossings, given by the code $\{\{1,1,1\},\{1,1,1\},\{1,1,1\},\{1,1,1\}\}$, Figure 10a, we derive many new knots and links, among them the smallest basic polyhedron – Borromean rings 6^* (6_2^3) given by the code $\{\{-1,-1,-2\},\{-2,-1,-2\},\{-2,2,-2\},\{-1,-1,-1\}\}$, see Figure 11b, and the first non-alternating 3-component link $2,2,-2$ (6_3^3) given by the code $\{\{-1,-1,1\},\{-1,-1,1\},\{-2,2,-2\}, \{-2,2,-2\}\}$ shown on Figure 10b.
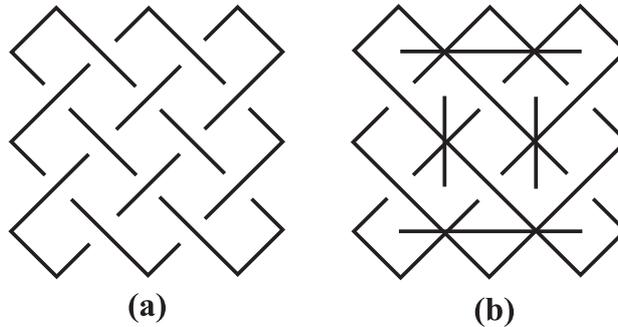

Figure 10: (a) $RG[3,3]$ with 3-component link $8^*2 : 2 : 2 : 2$ (b) non-alternating 3-component link $2,2,-2$ (6_3^3).

Alternating link $8^*2 : 2 : 2 : 2$ corresponds to $RG[3,3]$, to which we associate the following prime knots and links: $(2,2)(3\,1,-3\,1)$, $(-5\,1,2)(2,2)$, $6^* - 2.2. - 2 : 4$, $6^*3.2. - 3 : 2$, $6^* - 3. - 3\,0 :: -3\,0$, $2\,1\,2\,1\,1\,1\,2$ (10_{44}), $.4.2\,0$ (10_{85}), $4\,1\,2\,1\,2$ ($L10a_{99}$), $.3 : 3\,0$ ($L10a_{140}$), $6,2,2$ ($L10a_{145}$), $.2.3.2\,0$ ($L10a_{162}$), $8^*2 :: 2$ ($L10a_{163}$), $2\,0.2.2\,0.2\,0$ ($L10a_{164}$), $(2\,1,-2\,1)(2,2)$

$(L10n_{73})$, $(3\,1,-2)\,(2,2)\,(L10n_{85})$, $(2,2)\,(4,-2)\,(L10n_{86})$, $4,3\,1,-2\,(L10n_{92})$, $4,4,-2\,(L10n_{93})$, $2\,0.-2.-2\,0.2\,0\,(L10n_{94})$, $3\,1,3\,1,-2\,(L10n_{95})$, $4\,1\,2\,2\,(9_{11})$, $4\,1\,1\,1\,2\,(9_{14})$, $2\,1\,3\,1\,2\,(9_{17})$, $2\,2\,1\,2\,2$ (9_{23}), $2\,1\,2\,1\,1\,2\,(9_{27})$, $2\,1\,1\,1\,1\,1\,2\,(9_{31})$, $6\,1\,2\,(9_1^2)$, $2\,2\,1\,1\,1\,2\,(9_{12}^2)$, $5,2,2\,(9_{13}^2)$, $.4\,(9_{31}^2)$, $.3.2\,0$ (9_{35}^2), $8^*2\,(9_{42}^2)$, $6\,2\,(8_1)$, $3,3,2\,(8_5)$, $4\,1\,1\,2\,(8_7)$, $2\,3\,1\,2\,(8_8)$, $2\,1,3,2\,(8_{10})$ $2\,2\,2\,2\,(8_{12})$ $2\,2\,1\,1\,2$ (8_{14}), $.2.2\,0\,(8_{16})$, $.2.2\,(8_{17})$, $8^*\,(8_{18})$, $2\,1\,2\,1\,2\,(8_7^2)$, $2\,1\,1\,1\,1\,2\,(8_8^2)$, $4,2,2\,(8_1^3)$, $3\,1,2,2\,(8_2^3)$, $(2,2)\,(2,2)\,(8_3^3)$, $.3\,(8_5^3)$, $.2:2\,0\,(8_6^3)$, $4,2,-2\,(8_7^3)$, $3\,1,2,-2\,(8_8^3)$, $(2,2)\,(2,-2)\,(8_9^3)$, $(2,2)-(2,2)$ (8_{10}^3), $4\,3\,(7_3)$, $3\,2\,2\,(7_5)$, $2,2,2+\,(7_1^3)$, $2\,3\,2\,(7_3^2)$, $3,2,2\,(7_4^2)$, $2\,1,2,2\,(7_5^2)$, $.2\,(7_6^2)$, $2,2,2\,(6_1^3)$, 6^* (6_2^3), and $2,2,-2\,(6_3^3)$.

5. Knot mosaics, mirror-curves, grid diagram representations and tame knot theory

Mirror-curves are equivalent to link mosaics: every link mosaic can be easily transformed into a mirror-curve and *vice versa*. For example, the mosaics of the figure-eight knot [23] (pp. 6) and Borromean rings [23] (pp. 7) correspond to the mirror-curves on Figure 11 and *vice versa*. Even more illustrative are knot mosaics from the paper [12] (pp. 15): first we rotate them by 45°, cut out the empty parts, and add the two-sided mirrors in appropriate places.
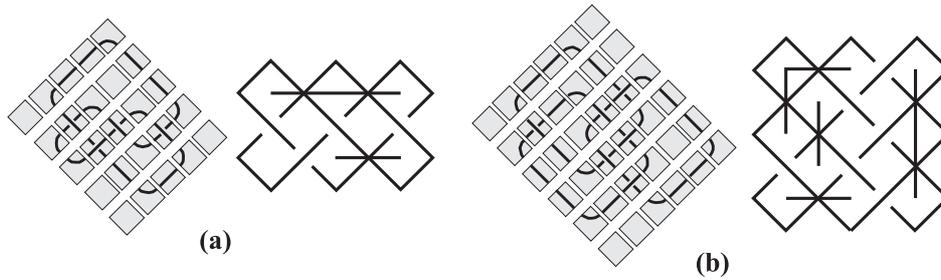

(a)   **(b)**

Figure 11: (a) Figure-eight knot and (b) Borromean rings from the paper [23] transformed into mirror-curves.

T. Kuriya [22] proved Lomonaco-Kauffman Conjecture [23], showing that the tame knots are equivalent to knot mosaics, hence also to mirror-curves. According to the Proposition 8.4 [22] there is a correspondence between knot mosaics and grid diagrams [3, 7, 24], that extends to mirror-curves.

The mosaic number $m(L)$ of a link L is the smallest number n for which L is representable as a link n-mosaic [22].

Theorem 4. *For every link L, the mosaic number $m(L) = p + q$, where p and q are dimensions of the minimal $RG[p,q]$ in which L can be realized. The dimension of the grid (arc) representation equals $m(L) + 1 = p + q + 1$.*

Conjecture 10.4 [22] is an easy corollary of this theorem, claiming that the mosaic number of the knot $2\,1\,1\,2\,(6_3)$ is 6, since its minimal rectangular grid is $RG[3,3]$, and its code is $\{\{2,-2,1\},\{1,1,-2\},\{-2,-2,-2\},\{1,1,1\}\}$ (Figure 12).

Notice that the knot $2\,1\,1\,2\,(6_3)$ does not cover $RG[3,3]$ entirely– if a square in our grid contains just a curl (kink) which can be undone with the Reidemeister I move, we call it empty square or a hole. Hence, it may be useful to look at the minimal size of every mirror-curve, i.e., the minimal number of non-empty squares necessary to draw it in some (hollow) polyomino [17].
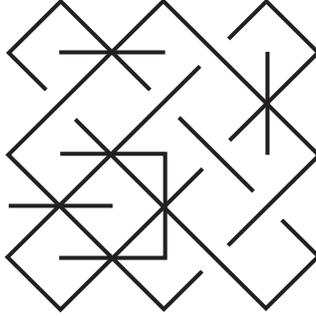
9

Figure 12: Mirror-curve diagram of the knot 2 1 1 2 (6_3) in $RG[3, 3]$.

Conjecture 1. *Mosaic number of a connected sum $L_1 \# L_2$ of two links L_1 and L_2 satisfies the following equality:*

$$m(L_1 \# L_2) = m(L_1) + m(L_2) - 3.$$

There are two additional numbers that potentially describe the structure of mirror-curves related to the unknotting (unlinking) number:

- the minimal number of two-sided mirrors that we need to add to some mirror-curve in order to obtain unlink,

- maximal number of mirrors that can be added to it without obtaining unlink.

For example, for a $RG[p, 2]$ ($p \geq 2$) the first number equals $p - 1$, and the other equals $3p - 4$.

6. Product of mirror-curves

Algebraic operation called *product* can be defined for mirror-curves derived from the same rectangular grid $RG[p, q]$ by promoting symbols 2, −2, 1, and −1 in their codes to elements of a semigroup of order 4 [26]. For example, consider the semigroup S of order 4, generated by elements $A = \{a, aba\}$, $B = \{b, bab\}$, $C = \{ab\}$, and $D = \{ba\}$, with the semigroup operation given in the Cayley table:

*	A	B	C	D
A	A	C	C	A
B	D	B	B	D
C	A	C	C	A
D	D	B	B	D

First, we substitute $2 \to a$, $-2 \to b$, $1 \to ab$, $-1 \to ba$, use the semigroup product and then substitute the original symbols back (Figure 13), to obtain the code $M_1 * M_2 = \{\{-2, -2, 1, 1\}, \{2, 1\}, \{-2, 2\}, \{-1, -1\}\}$ as the product of mirror-curves $M_1 = \{\{-2, -2, 1, 1\}, \{1, 2\}, \{-1, 1\}, \{-1, -2\}\}$ and $M_2 = \{\{-2, -2, 1, 1\}, \{-1, -2\}, \{1, -1\}, \{2, -1\}\}$ (Figure 14).

Since the elements a, b, ab and ba are idempotents, we have the equality $M * M = M^2 = M$ for every mirror-curve M. If $M_{[p,q]}$ is the set of all mirror-curves derived from $RG[p, q]$, the basis (minimal set of mirror-curves from which $M_{[p,q]}$ can be obtained by the operation of product) is
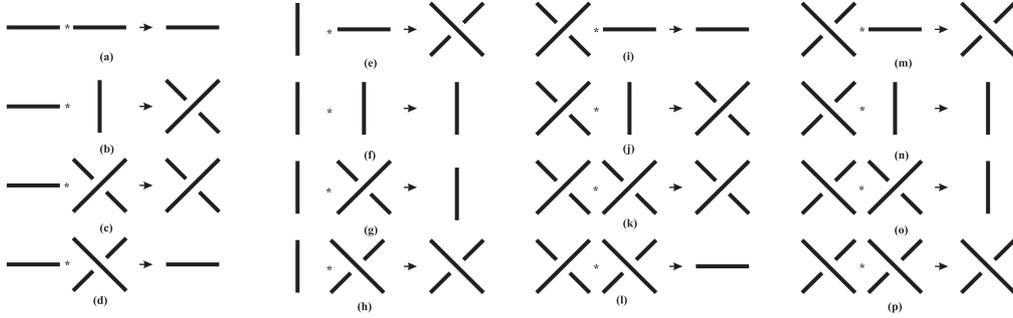
Figure 13: (a) $2 * 2 \rightarrow 2$; (b) $2 * -2 \rightarrow 1$; (c) $2 * 1 \rightarrow 1$; (d) $2 * -1 \rightarrow 2$; (e) $-2 * 2 \rightarrow -1$; (f) $-2 * -2 \rightarrow -2$; (g) $-2 * 1 \rightarrow -2$; (h) $-2 * -1 \rightarrow -1$; (i) $1 * 2 \rightarrow 2$; (j) $1 * -2 \rightarrow 1$; (k) $1 * 1 \rightarrow 1$; (l) $1 * -1 \rightarrow 2$; (m) $-1 * 2 \rightarrow -1$; (n) $-1 * -2 \rightarrow -2$; (o) $-1 * 1 \rightarrow -2$; (p) $-1 * -1 \rightarrow -1$.

the subset of all mirror-curves of dimensions $p \times q$ with codes consisting only of 2's and -2's (Figure 15), i.e. the set of all unlinks belonging to $RG[p, q]$. The basis is not closed under the operation of product: the product of two mirror-curves belonging does not belong to the same basis, since it has at least one crossing.
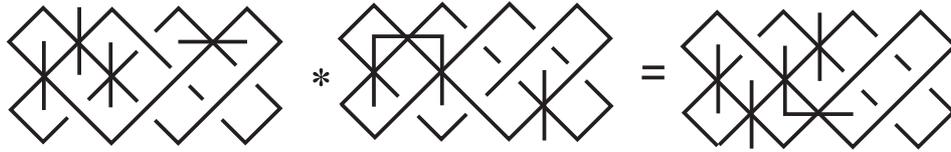

Figure 14: Product $M_1 * M_2 = \{\{-2, -2, 1, 1\}, \{2, 1\}, \{-2, 2\}, \{-1, -1\}\}$ of mirror-curves $M_1 = \{\{-2, -2, 1, 1\}, \{1, 2\}, \{-1, 1\}, \{-1, -2\}\}$ and $M_2 = \{\{-2, -2, 1, 1\}, \{-1, -2\}, \{1, -1\}, \{2, -1\}\}$.
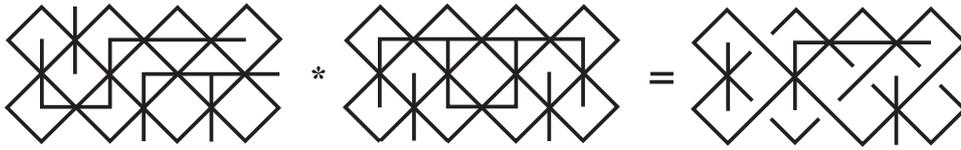
Figure 15: Product $M_1 * M_2 = \{\{-2, -2, 1, 1\}, \{-1, 1\}, \{1, -2\}, \{2, -2\}\}$ of mirror-curves $M_1 = \{\{-2, -2, 2, 2\}, \{-2, 2\}, \{2, -2\}, \{2, -2\}\}$ and $M_2 = \{\{-2, -2, -2, -2\}, \{2, -2\}, \{-2, -2\}, \{2, -2\}\}$.

In particular, alternating knot or link corresponding to $RG[p, q]$ is obtained as the product of mirror-curves containing only vertical and horizontal mirrors, see Figure 16. Substituting with elements of different semigroups of order 4 listed in [11], we could obtain different multiplication laws for mirror-curves.

7. Kauffman bracket polynomial and mirror-curves

Let L be any unoriented link diagram. Define the *Kauffman state S* of L to be a choice of smoothing for each crossing of L [18, 19, 20]. There are two choices of smoothing for each crossing, A-smoothing and B-smoothing, and thus there are 2^c states of a diagram with c crossings. In

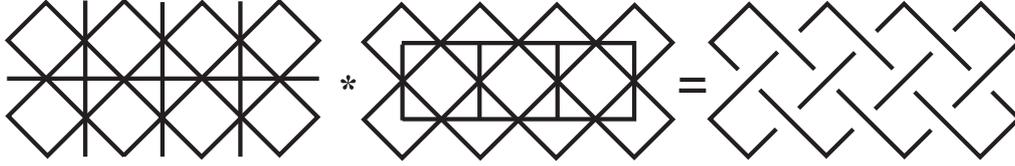Figure 16: Alternating link 3 1 2 1 3 ($L10a_{101}$) corresponding to $RG[4, 2]$ obtained as the product $M_1 * M_2 = \{\{1, 1, 1, 1\}, \{1, 1\}, \{1, 1\}, \{1, 1\}\}$ of mirror-curves $M_1 = \{\{2, 2, 2, 2\}, \{2, 2\}, \{2, 2\}, \{2, 2\}\}$ and $M_2 = \{\{-2, -2, -2, -2\}, \{-2, -2\}, \{-2, -2\}, \{-2, -2\}\}$.

a similar way, we can define the Kauffman state of $RG[p, q]$ as a mirror-curve in $RG[p, q]$ whose code contains only 2's and −2's.

Let us consider the set $M^*_{[p,q]}$, called the Kauffman states of $RG[p, q]$, which contains 2^v elements corresponding to the choice of mirrors 2 or −2 in the mid-points of $v = 2pq - p - q$ internal edges of $RG[p, q]$. Every element of $M^*_{[p,q]}$ can be characterized by the dimensions p and q of the grid $RG[p, q]$, and another integer m ($0 \leq m \leq 2^v - 1$). In order to obtain the matrix code of some mirror-curve from (p, q, m) code, substitute 0 by 2 and 1 by −2 in the binary expansion of m then subdivide the list into $q - 1$ lists of length p and $p - 1$ lists of length q. This code naturally extends to products of mirror-curves. Every mirror-curve M in $RG[p, q]$ can be represented as a product $M = M_1 * M_2$ of two mirror-curves M_1 and M_2 from the set $M^*_{[p,q]}$, hence it can be denoted by a four-number code (p, q, m, n), compounded from codes (p, q, m) and (p, q, n) of mirror-curves (Kauffman states) M_1 and M_2, respectively.

For example, the mirror-curve M corresponding to a trefoil knot in $RG[2, 2]$ can be represented by the code $(2, 2, 1, 15)$. By expressing numbers $m = 1$ and $n = 15$ in 4-digit binary codes, we obtain $\{0, 0, 0, 1\}$ and $\{1, 1, 1, 1\}$, so M is the product of the mirror-curves $\{\{2, 2\}, \{2, -2\}\}$ and $\{\{-2, -2\}, \{-2, -2\}\}$. Four-number code is not unique. For example, a trefoil in $RG[2, 2]$ can be represented by $(2, 2, 1, 15)$, $(2, 2, 2, 15)$, $(2, 2, 4, 15)$, and $(2, 2, 8, 15)$. We choose the minimal code $(2, 2, 1, 15)$ as the code of the trefoil knot.

This approach provides an easy algorithm for computing the Kauffman bracket polynomial [18, 19, 20] of an alternating link L directly from its mirror-curve representation. The Kauffman state sum approach bypasses the recursive skein relation definition of the Kauffman bracket polynomial, which is given by the formula

$$\sum_S a^{A(S)} a^{-B(S)} (-a^2 - a^{-2})^{|S|-1},$$

as the sum over all Kauffman states S of a link L, where $A(S)$ and $B(S)$ is the number of A-smoothings and B-smoothings, respectively, and $|S|$ is the number of components in the particular state [18, 19].

Analogously, the Kauffman bracket polynomial can be computed as the sum of all possible states of the mirror-curve representing our link L.

Since all Kauffman states of a link L represented by a mirror-curve M in a grid $R[p, q]$ form a subset of $M^*_{[p,q]}$, the Kauffman bracket polynomial can be computed from the data associated to the mirror-curves in $M^*_{[p,q]}$. Let M_i be a mirror-curve corresponding to some Kauffman state S_i of a link L. Denote by A_i be the number of mirrors labeled 1 in M that changed to 2 in M_i, and $|M_i|$ be the number of components of a Kauffman state M_i. Then the bracket polynomial of
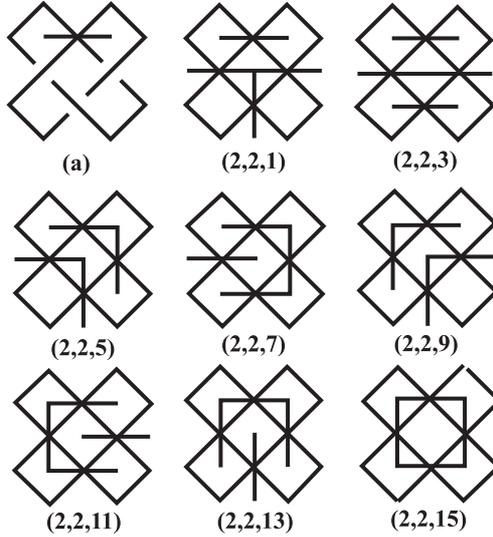
Figure 17: Computation of the Kauffman bracket polynomial for a trefoil.

L can be expressed as

$$< M >= \sum_{i=0}^{2^n-1} a^{A_i} a^{-n+A_i} (-a^2 - a^{-2})^{|M_i|-1} \qquad (1)$$

For example, a trefoil given by the mirror-curve $(2, 2, 1, 15) = \{\{1, 1\}, \{1, -2\}\}$, shown in Figure 17a, has 8 states: $\{\{2, 2\}, \{2, -2\}\}$, $\{\{2, 2\}, \{-2, -2\}\}$, $\{\{2, -2\}, \{2, -2\}\}$, $\{\{2, -2\}, \{-2, -2\}\}$, $\{\{-2, 2\}, \{2, -2\}\}$, $\{\{-2, 2\}, \{-2, -2\}\}$, $\{\{-2, -2\}, \{2, -2\}\}$, $\{\{-2, -2\}, \{-2, -2\}\}$ given by the codes $(2, 2, 2k + 1)$, $0 \le k \le 7$, see Figure 17.

According to the multiplication table shown on Figure 13), a mirror image of a link L given as a product mirror-curve $M = M_1 * M_2$, is $M' = M_2 * M_1$. If $M = M_1 * M_2$, the pair of mirror-curves (M_1, M_2) will be called the *decomposition* of M. Minimal decomposition yields the minimal mirror-curve code (p, q, m, n) for every link L. For example, the Hopf link is given by the minimal (p, q, m, n)-code $(2, 2, 1, 14)$, trefoil by $(2, 2, 1, 15)$, figure-eight knot by $(3, 2, 7, 127)$, *etc.*

To facilitate computations of the Kauffman bracket polynomial we use two special Kauffman states with all smoothings of one kind: A-state (B-state) that contain only A-smoothings (B-smoothings)[3].

Let us denote by $M_0 = (p, q, 0)$ the A-state, and by $M_{2^v-1} = (p, q, 2^v - 1)$ the B-state of $RG[p, q]$.

Theorem 5. *Every representation of an alternating link L as a mirror-curve in $RG[p, q]$ can be given as a (left or right) product of some Kauffman state M with M_0 or M_{2^v-1}, determined by a code $(p, q, m, 2^v - 1)$ or $(p, q, 0, n)$, with $v = 2pq - p - q$ and $m, n \in \{0, 2^v - 1\}$.*

---

[3]In the language of the Kauffman states of mirror-curves, this means that the first contains only 2's, and the other −2's.

Such a representation of an alternating link L will be called *canonical representation*. For example, the minimal representation of the Hopf link is $(2, 2, 1, 14)$, and its canonical representation is $(2, 2, 5, 15)$. The minimal and canonical representation of an alternating link cannot always be obtained from the same rectangular grid. Similarly, the minimal representation of the knot $4\,2$ (6_1) can be obtained from $RG[3, 2]$, and its first canonical representation from $RG[4, 2]$.

Every non-alternating mirror-curve M in $RG[p, q]$ can be uniquely represented as the product of two alternating mirror-curves $M_1 = (p, q, m_1, n_1)$ and $M_2 = (p, q, m_2, n_2)$. This means that every non-alternating link L or an alternating link given by its non-alternating mirror-curve diagram can be denoted by the minimal code of the form $(p, q, m_1, n_1, m_2, n_2)$.

In order to compute the Kauffman bracket polynomial of non-alternating links from mirror-curves we can use the preceding results obtained for alternating mirror-curves and extend our computation to all mirror-curves by using skein relation for bracket polynomial, i.e., the product of mirror-curves. For example, consider a non-alternating link $2, 2, -2$ (6_3^3) in $RG[3, 3]$, given by the code $M = \{\{1, 1, -1\}, \{1, 1, -1\}, \{-2, 2, -2\}, \{-2, 2, -2\}\}$. Let $< M >$ denote the bracket polynomial of the mirror-curve M. Then:

$$
\begin{aligned}
< M > \ &= \ a(a < M_0 > + a^{-1} < M_1 >) + a^{-1}(a < M_2 > + a^{-1} < M_3 >) \\
&= \ a^2 < M_0 > + < M_1 > + < M_2 > + a^{-2} < M_3 >,
\end{aligned}
$$

where

$$
\begin{aligned}
M_0 \ &= \ \{\{1, 1, -2\}, \{1, 1, -2\}, \{-2, 2, -2\}, \{-2, 2, -2\}\}, \\
M_1 \ &= \ \{\{1, 1, -2\}, \{1, 1, 2\}, \{-2, 2, -2\}, \{-2, 2, -2\}\}, \\
M_2 \ &= \ \{\{1, 1, 2\}, \{1, 1, -2\}, \{-2, 2, -2\}, \{-2, 2, -2\}\}, \\
M_3 \ &= \ \{\{1, 1, 2\}, \{1, 1, 2\}, \{-2, 2, -2\}, \{-2, 2, -2\}\}
\end{aligned}
$$

are mirror-curves with all crossings positive. Hence,

$$
\begin{aligned}
< M > \ &= \ a^2(2 + a^{-8} + a^8) + (-a^{-6} - a^2 + a^6 - a^{10}) + (-a^{-6} - a^2 + a^6 - a^{10}) + \\
&\quad a^{-2}(1 + a^{-8} + a^{-4} + a^{12}) = a^{-10} + a^{-2} + 2a^6.
\end{aligned}
$$

Notice that we have used all Kauffman states, this time expanded over all negative crossings. In the case of a non-alternating mirror-curve M with n crossings, and n_- negative crossings the Kauffman bracket polynomial is given by the following state sum formula:

$$
< M > = \sum_{i=0}^{2^n - 1} a^{A_i} a^{-n_- + A_i} < M_i >, \tag{2}
$$

where A_i is the number of mirrors changed from 1 in M to -2 in a Kauffman state M_i, and M_i ($0 \le i \le 2^n - 1$) are alternating mirror-curves obtained as the Kauffman states taken over negative crossings by changing -1 into -2 and 2. Since every mirror-curve M_i corresponding to some Kauffman state S_i is just a collection of $|M_i| = |S_i|$ circles, its Kauffman bracket is $< M_i > = (-a^2 - a^{-2})^{|S_i| - 1}$. Moreover, the power of $a^{A_i} a^{-n_- + A_i}$ is the vertex weight w_i: the number of A-smoothings minus the number of B smoothings in a state S_i times ± 1, depending on the sign of each crossing. The state sum formula for the Kauffman bracket polynomial [19] now has the following form:

$$
\sum_{i=0}^{2^n - 1} a^{w_i} (-a^2 - a^{-2})^{|S_i| - 1} \tag{3}
$$

Kauffman state $M_i = S_i$	$|M_i| = |S_i|$
$M_0 = \{\{-2, -2\}, \{2, -2\}\}$	1
$M_1 = \{\{-2, -2\}, \{-2, -2\}\}$	2
$M_2 = \{\{-2, 2\}, \{2, -2\}\}$	2
$M_3 = \{\{-2, 2\}, \{-2, -2\}\}$	1
$M_4 = \{\{2, -2\}, \{2, -2\}\}$	2
$M_5 = \{\{2, -2\}, \{-2, -2\}\}$	1
$M_6 = \{\{2, 2\}, \{2, -2\}\}$	3
$M_7 = \{\{2, 2\}, \{-2, -2\}\}$	2

Table 1: 2^n mirror-curves M_i ($i = 0, \ldots, 2^n - 1$) shown on Figure 18 and the number of their link components.

Example 6. *To illustrate the formula above, we give an explicit computation of the Kauffman bracket using the formula above, for the mirror-curve $M = \{\{1, 1\}, \{-1, -2\}\}$ shown on Figure 18a, which is just an unknot represented as a trefoil with one crossing change.*
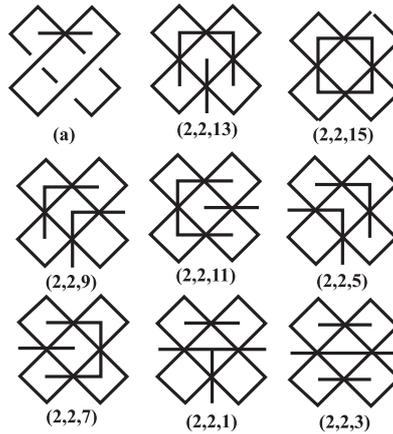
Figure 18: Computation of the Kauffman bracket polynomial for the mirror-curve $M = \{\{1, 1\}, \{-1, -2\}\}$ (a) and its eight states.

Eight mirror-curves M_i corresponding to the Kauffman states S_i, $i = 0, \ldots, 7$ are shown on Figure 18 and their codes, as well as the number of components, are contained in Table 1. Next we compute the vertex weights $(w_0, \ldots, w_7) = (3, 1, 1, -1, 1, -1, -1, -3)$, to obtain $< M >= -a^3$.

8. L-polynomials and mirror-curves

Mirror-curves can also be used for computing the Kauffman L-polynomial [19, 20] defined by the following axioms:

1. $L(+1) + L(-1) = z(L(0) + L(\infty))$;
2. $L \leftrightthreetimes = aL$;
3. $L \leftrightharpoons = a^{-1}L$;

4. $L(\bigcirc) = 1$;

where ↬ and ↫ denote positive and negative curls.

Figure 19: Mirror-curves obtained from $RG[2, 2]$ up to isometry.

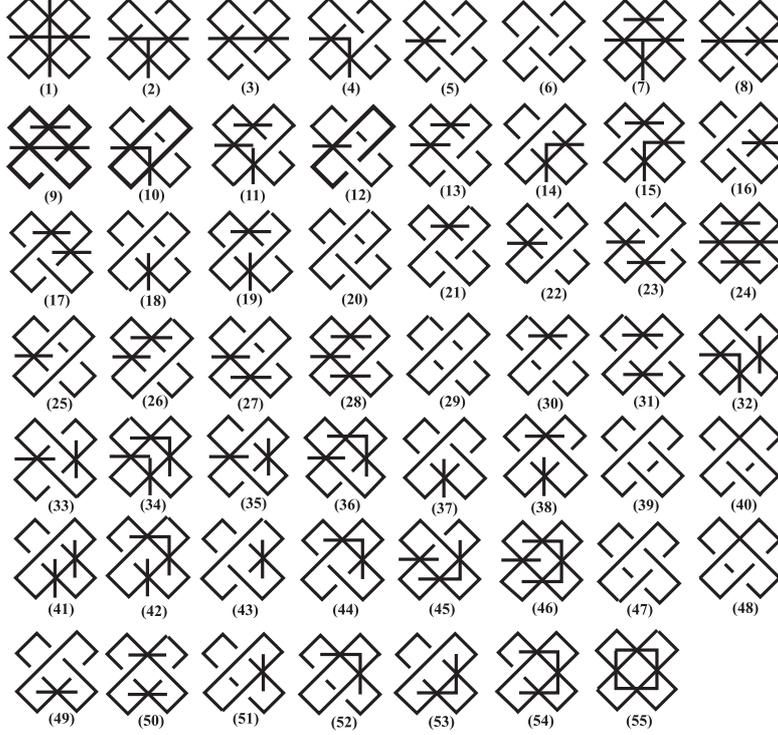Grid $RG[2, 2]$ contains 55 mirror-curves[4] shown on Figure 19), where the mirror-curves (20) and (47) reduce to (44), (23) and (52) reduce to (55), (50) reduces to (24), and (30) reduces to (54). Knowing that $L(\bigcirc^n) = \delta^{n-1}$, where $\delta = (\frac{a+a^{-1}}{z} - 1)$, we can compute the L-polynomial for all of them except for the mirror-curves (6), (21), (31) and (44) by simply counting circles and curls.

We have the following relations which are also illustrated on Figure 20:

$$L(\{\{1, 1\}, \{-2, -2\}\}) + L(\{\{1, -1\}, \{-2, -2\}\}) = z(L(\{\{1, 2\}, \{-2, -2\}\}) + L(\{\{1, -2\}, \{-2, -2\}\})),$$

with $L(\{\{1, -1\}, \{-2, -2\}\}) = L(\{\{2, 2\}, \{-2, -2\}\})$.

In other words, we have $L(31) + L(50) = z(L(28) + L(54))$, with $L(50) = L(24)$.

$$L(\{\{1, -2\}, \{1, -2\}\}) + L(\{\{1, -2\}, \{-1, -2\}\}) = z(L(\{\{1, -2\}, \{2, -2\}\}) + L(\{\{1, -2\}, \{-2, -2\}\})),$$

where $L(\{\{1, -2\}, \{-1, -2\}\}) = L(\{\{-2, -2\}, \{-2, -2\}\})$, i.e., $L(44) + L(52) = z(L(42) + L(54))$, with $L(52) = L(55)$:

$$L(\{\{1, 1\}, \{1, -2\}\}) + L(\{\{1, 1\}, \{-1, -2\}\}) = z(L(\{\{1, 1\}, \{2, -2\}\}) + L(\{\{1, 1\}, \{-2, -2\}\})).$$
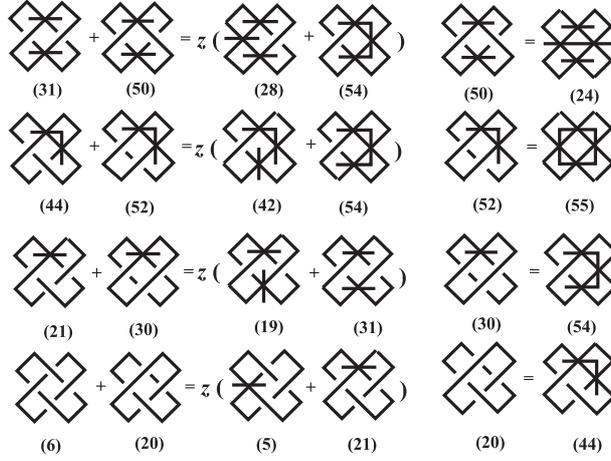
---

[4]Up to isometry.

Figure 20: Computation of L-polynomial from mirror-curves in $RG[2, 2]$.

with $L(\{\{1, 1\}, \{-1, -2\}\}) = L(\{\{1, -2\}, \{-2, -2\}\})$, i.e., $L(21) + L(30) = z(L(19) + L(31))$. Since $L(30) = L(54)$ we have

$$L(\{\{1, 1\}, \{1, 1\}\}) + L(\{\{1, 1\}, \{1, -1\}\}) = z(L(\{\{1, 1\}, \{1, 2\}\}) + L(\{\{1, 1\}, \{1, -2\}\})),$$

with $L(\{\{1, 1\}, \{1, -1\}\}) = L(\{\{1, -2\}, \{1, -2\}\})$ i.e., $L(6) + L(20) = z(L(5) + L(21))$, with $L(20) = L(44)$, see Figure 20.
Hence, we conclude that

$$
\begin{aligned}
L(Hopf\ Link) &= L(2_1^2) = L(31) = z(L(28) + L(54)) - L(24) = z(a^{-1} + a) - \delta^2 \\
&= -(a^{-1} + a)z^{-1} + 1 + (a^{-1} + a)z, \\
L(Right\ Trefoil) &= L(3_1) = L(21) = z(L(19) + L(31)) - L(54) = z(a^{-2} + L(31)) - a = \\
&= -(a^{-1} + 2a) + (a^{-2} + 1)z + (a^{-1} + a)z^2, \\
L(4_1^2) &= L(6) = z(L(5) + L(21)) - L(44) = z(a^{-3} + L(21)) - L(44) \\
&= -(a^{-1} + a)z^{-1} - 1 + (a^{-3} - 2a^{-1} - 3a)z + (a^{-2} + 1)z^2 + (a^{-1} + a)z^3.
\end{aligned}
$$

In general, L-polynomials for mirror-curves can be computed in the same way, or by simplifying computations using previously obtained results and relations. For example, the L-polynomial of the mirror-curve, see Figure 21, $\{\{-2, 1, 1\}, \{1, 1\}, \{-2, -2\}\}$ which represents the figure-eight knot 4_1 in $RG[3, 2]$ satisfies the relation:

$$L(\{\{-2, 1, 1\}, \{1, 1\}, \{-2, -2\}\}) + L(\{\{-2, 1, 1\}, \{1, -1\}, \{-2, -2\}\})) =$$
$$z(L(\{\{-2, 1, 1\}, \{1, 2\}, \{-2, -2\}\}) + L(\{\{-2, 1, 1\}, \{1, -2\}, \{-2, -2\}\}))$$

Since $L(\{\{-2, 1, 1\}, \{1, -1\}, \{-2, -2\}\}) = a^{-2}$, $L(\{\{-2, 1, 1\}, \{1, 2\}, \{-2, -2\}\}) = aL(31)$, and the mirror-curve $\{\{-2, 1, 1\}, \{1, -2\}, \{-2, -2\}\}$ reduces to $\{\{1, 1\}, \{-2, 1\}\} = \{\{1, 1\}, \{-2, 1\}\}$, i.e., to the mirror-curve (21) in $RG[2, 2]$ corresponding to the trefoil knot,

$$
\begin{aligned}
L(4_1) &= z(aL(31) + L(21)) - a^{-2} = (-a^{-2} - 1 - a^2) - (a^{-1} + a)z + \\
&\quad (a^{-2} + 2 + a^2)z^2 + (a^{-1} + a)z^3.
\end{aligned}
$$

17

Figure 21: Computation of L-polynomial for figure-eight knot.

This approach can also be used for deriving recursive formulas relating the L-polynomials of knot and link families given in Conway notation. Members of the knot family p ($p \geq 1$), denoted by Conway symbols as 1, 2, 3, 4, 5, . . ., namely the unknot, Hopf link 2_1^2, trefoil 3_1, link 4_1^2, knot 5_1, . . . satisfy the following recursion:

$$
\begin{aligned}
L(1) &= a \\
L(2) &= -(a^{-1} + 2a) + (a^{-2} + 1)z + (a^{-1} + a)z^2 \\
L(p) &= z(a^{-p+1} + L(p-1)) - L(p-2), \quad \text{for } p \geq 3.
\end{aligned}
$$

For the knot family $p\,2$ ($p \geq 2$), which consists from knots 4_1, 5_2, 6_1, 7_2, . . . we have the recursion

$$
\begin{aligned}
L(1\,2) &= L(3) \\
L(2\,2) &= (-a^{-2} - 1 - a^2) - (a^{-1} + a)z + (a^{-2} + 2 + a^2)z^2 + (a^{-1} + a)z^3 \\
L(p\,2) &= z(L((p-1)\,2) + a^{p-1}L(2)) - L((p-2)\,2), \quad \text{for } p \geq 3.
\end{aligned}
$$

Members of the link family $3\,p$ ($p \geq 3$) satisfy the recursion

$$
L(3\,p) = z(L(2\,p) + a^2 L(p)) - L(p+1), \quad \text{for } p \geq 3,
$$

where $2\,p$ is the mirror image of the link $p\,2$, and $3\,p$ is the mirror image of the link $p\,3$.

In general, the link family $p\,q$ ($p \geq q \geq 2$) satisfies the following recursion

$$
L(p\,q) = z(L((p-1)\,q) + a^{p-1}L(q)) - L((p-2)\,q).
$$

References

[1] Ascher, M.: Ethnomathematics: A Multicultural View of Mathematical Ideas, Brooks & Cole, Pacific Grove (Ca), 1991.

[2] Baldwin, J. and Gillam, W.: Computations of Heegaard-Floer knot homology, arXiv:math.GT/0610167v3 (2007).

[3] Bar-Natan, D.: Knot Atlas, `http://katlas.math.toronto.edu/wiki/ Arc_Presentations`

[4] Chavey, D.: Symmetry groups of Tchokwe sand drawings, Symmetry: Culture and Science, **21**, 1–3 (2010) 191–206.

[5] Chavey, D.: Strip symmetry groups of African Sona designs, in Proceedings of the 13th Annual Conference of BRIDGES: Mathematical Connections in Art, Music, and Science (BRIDGES 2010), Pécs, Hungary, July 24-28, 2010, 111-118.

[6] Conway, J.: An enumeration of knots and links and some of their related properties, in Computational Problems in Abstract Algebra, Proc. Conf. Oxford 1967 (Ed. J. Leech), 329–358, Pergamon Press, New York, 1970.

[7] Cromwell, P. R.: Embedding knots and links in an open book I: Basic properties, Topology Appl. 64 (1995), 37–58.

[8] Culler, M.: *Gridlink*, `http://www.math.uic.edu/~culler/gridlink/`

[9] Damian, M., Demaine, E.D., Demaine, M.L., Dujmović, V., El-Khechen, D., Flatland, R. Iacono, J., Langerman, S., Meijer, H., Ramaswami,S., Souvaine, D.L., Taslakian, P., and Toussaint, G.T.: Curves in the sand: Algorithmic drawing. In Proceedings of the 18th Canadian Conference in Computational Geometry (CCCG06), Kingston, Canada, August 2006, 11-14.

[10] Demaine, E.D., Demaine, M.L., Taslakian, P. and Toussaint, G.T.: Sand Drawings and Gaussian Graphs, in Proceedings of the 9th Annual Conference of BRIDGES: Mathematical Connections in Art, Music, and Science (BRIDGES 2006), London, England, August 4-8, 2006, 79-88.

[11] Forsythe, G. E.: SWAC computes 126 distinct semigroups of order 4, Proceedings of the American Mathematical Society, **6**, 3 (1955) 443–447.

[12] Gerdes, P.: Reconstruction and extension of lost symmetries, *Comput. Math. Appl.*, **17**, 4–6 (1989) 791–813.

[13] Gerdes, P.: Lunda Geometry–Designs, Polyominoes, Patterns, Symmetries, Universidade Pedagógica Moçambique, Maputo, 1996.

[14] Gerdes, P.: On mirror curves and Lunda designs, Computers&Graphics **21**, 3 (1997), 371–378.

[15] Gerdes, P.: Geometry from Africa: Mathematical and Educational Explorations, Washington, DC: The Mathematical Association of America, (1999).

[16] Gerdes, P.: Sona Geometry from Angola: mathematics of an African tradition, Polimetrica International Scientific Publisher, Milan, Italy (2006).

[17] Golomb, S.: Polyominoes: Puzzles, Patterns, Problems, and Packings, Princeton University Press, Princeton (1994).

[18] Jablan, S. V. and Sazdanović, R.: *LinKnot- Knot Theory by Computer*. World Scientific, New Jersey, London, Singapore (2007) (`http://math.ict.edu.rs/`).

[19] Kauffman, L. H.: *Formal Knot Theory*. Dover Publications Inc., Mineola, New York (2006).

[20] Kauffman, L. H.: *On Knots*. Dover Annals of Mathematic Studies, No. 115, Princeton University Press, Princeton, New Jersey (1987).

[21] Kauffman, L. H.: Virtual Knot Theory, Europ. J. Combinatorics, **20** (1999), 663–691.

[22] Kuriya, T.: On a Lomonaco-Kauffman Conjecture, arXiv:math.GT/0811.0710v3 (2008).

[23] Lomonaco, S. J. and Kauffman, L. H.: Quantum knots and mosaics, Quantum Information Processing **7**, 2–3 (2008), 85–115 (arXiv:quant-ph/0805.0339v1).

[24] Manolescu, C., Ozsváth, P. Szábo, Z. and Thurston, D.: On combinatorial link Floer homology, arXiv:math.GT/0610559v2 (2007).

[25] Rolfsen, D.: Knots and Links, Publish & Perish Inc., Berkeley, 1976 (American Mathematical Society, AMS Chelsea Publishing, 2003).

[26] Tamura, T.: Note on a Semigroup Having No Proper Subsemigroup, Proceedings of the Japan Academy, **37**, 2 (1961) 72–74.

9. Appendix

1	3 1 2 1 3	$L10a_{101}$	$\{\{-1,-1,-1,-1\},\{-1,-1\},\{-1,-1\},\{-1,-1\}\}$
2	5 1 3	9_5	$\{\{-1,2,-1,-1\},\{-1,-1\},\{-1,-1\},\{-1,-1\}\}$
3	3 1 2 1 2	9_{20}	$\{\{-2,-1,-1,-1\},\{-1,-1\},\{-1,-1\},\{-1,-1\}\}$
4	4 1 1 3	9_5^2	$\{\{-1,-1,1,1\},\{-1,-1\},\{-1,-1\},\{1,1\}\}$
5	3 1 3 2	9_8^2	$\{\{-1,-1,-1,1\},\{-1,-1\},\{-1,-1\},\{1,1\}\}$
6	3 1 1 1 3	9_9^2	$\{\{-1,-1,-1,-1\},\{-1,-1\},\{-2,-1\},\{-1,-1\}\}$
7	5 1 2	8_2	$\{\{-2,-1,2,-1\},\{-1,-1\},\{-1,-1\},\{-1,-1\}\}$
8	4 1 3	8_4	$\{\{-2,2,-1,-1\},\{-1,-1\},\{-1,-1\},\{-1,-1\}\}$
9	3 1 1 1 2	8_{13}	$\{\{-2,-1,-1,-1\},\{-1,-1\},\{-2,-1\},\{-1,-1\}\}$
10	8	8_1^2	$\{\{-1,2,2,-1\},\{-1,-1\},\{-1,-1\},\{-1,-1\}\}$
11	4 2 2	8_3^2	$\{\{-1,1,-1,-1\},\{-1,-1\},\{1,1\},\{-1,-1\}\}$
12	3 2 3	8_4^2	$\{\{-1,-1,-1,-1\},\{-1,-1\},\{-1,1\},\{-1,-1\}\}$
13	3 1 2 2	8_5^2	$\{\{-2,-1,-1,-1\},\{-2,-1\},\{-1,-1\},\{-1,-1\}\}$
14	2 4 2	8_6^2	$\{\{-1,1,1,-1\},\{-1,-1\},\{1,1\},\{-1,-1\}\}$
15	2 1 2 1 2	8_7^2	$\{\{-2,-1,-1,-2\},\{-1,-1\},\{-1,-1\},\{-1,-1\}\}$
16	7	7_1	$\{\{-2,2,2,-1\},\{-1,-1\},\{-1,-1\},\{-1,-1\}\}$
17	5 2	7_2	$\{\{-2,-1,2,-1\},\{-2,-1\},\{-1,-1\},\{-1,-1\}\}$
18	2 2 1 2	7_6	$\{\{-2,-1,-1,-2\},\{-2,-1\},\{-1,-1\},\{-1,-1\}\}$
19	2 1 1 1 2	7_7	$\{\{-2,-1,-1,-2\},\{-1,-1\},\{-2,-1\},\{-1,-1\}\}$
20	4 1 2	7_1^2	$\{\{-2,2,-1,-2\},\{-1,-1\},\{-1,-1\},\{-1,-1\}\}$
21	3 1 1 2	7_2^2	$\{\{-1,-1,-1,-2\},\{-1,-1\},\{-2,-1\},\{-2,-1\}\}$
22	2 3 2	7_3^2	$\{\{1,-1,-1,1\},\{-1,-1\},\{-1,-1\},\{1,1\}\}$
23	2 1 1 2	6_3	$\{\{-2,-1,-1,-2\},\{-1,-1\},\{-2,-1\},\{-2,-1\}\}$
24	3 3	6_2^2	$\{\{-1,1,-1,-1\},\{-1,-1\},\{-1,-1\},\{-1,-1\}\}$
25	2 2 2	6_3^2	$\{\{-2,-1,-1,-2\},\{-2,-1\},\{-1,-1\},\{-2,-1\}\}$

Table 2: *KL*s derived from $RG[4, 2]$
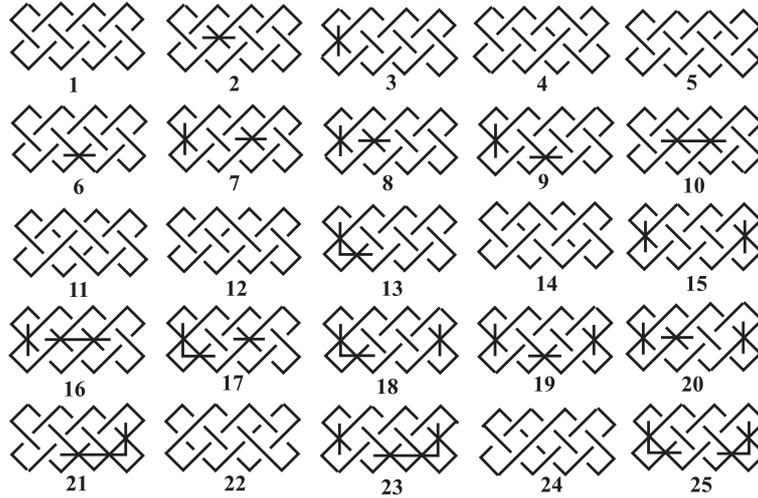
Figure 22: Mirror-curves 1-25 derived from $RG[4, 2]$.

|			
1	$8^*2 : 2 : 2$		$\{\{-1,-1,-1\},\{-1,-1,-1\},\{-1,-1,-1\},\{-1,-1,-1\}\}$
2	$(2,2)(3\,1,-3\,1)$		$\{\{-1,1,1\},\{-1,-1,-1\},\{-1,-1,-1\},\{1,1,-1\}\}$
3	$(-5\,1,2)(2,2)$		$\{\{-1,-1,1\},\{-1,-1,-1\},\{-1,-1,-1\},\{1,1,1\}\}$
4	$6^* - 2.2. - 2 : 4$		$\{\{-1,-1,1\},\{1,-1,-1\},\{-1,-1,1\},\{1,-1,-1\}\}$
5	$6^*3.2. - 3 : 2$		$\{\{1,1,1\},\{-1,-1,-1\},\{1,-1,-1\},\{1,-1,-1\}\}$
6	$6^* - 3. - 3\,0 :: -3\,0$		$\{\{-1,1,-1\},\{-1,1,-1\},\{-1,1,-1\},\{-1,1,-1\}\}$
7	$2\,1\,2\,1\,1\,1\,2$	10_{44}	$\{\{-1,-1,-1\},\{-2,-1,-1\},\{-1,-1,-1\},\{-1,-2,-1\}\}$
8	$.4.2\,0$	10_{85}	$\{\{-1,-1,-1\},\{-2,-1,-1\},\{-1,-1,-1\},\{-1,2,-1\}\}$
9	$4\,1\,2\,1\,2$	$L10a_{99}$	$\{\{-1,-1,-1\},\{-1,-2,-1\},\{-1,-1,-1\},\{-1,2,-1\}\}$
10	$.3 : 3\,0$	$L10a_{140}$	$\{\{1,1,1\},\{-1,-1,-1\},\{1,1,1\},\{1,-1,-1\}\}$
11	$6,2,2$	$L10a_{145}$	$\{\{-1,-1,-1\},\{-1,2,-1\},\{-1,-1,-1\},\{-1,2,-1\}\}$
12	$.2.3.2\,0$	$L10a_{162}$	$\{\{-1,-1,1\},\{-1,-1,-1\},\{-1,-1,-1\},\{1,1,1\}\}$
13	$8^*2 :: 2$	$L10a_{163}$	$\{\{-1,-1,-1\},\{-2,-1,-1\},\{-1,-1,-1\},\{-2,-1,-1\}\}$
14	$2\,0.2\,0.2\,0$	$L10a_{164}$	$\{\{-1,-1,1\},\{-1,-1,-1\},\{-1,-1,-1\},\{-1,-1,-1\}\}$
15	$(2\,1,-2\,1)(2,2)$	$L10n_{73}$	$\{\{1,1,1\},\{1,-1,-1\},\{1,-1,-1\},\{1,-1,-1\}\}$
16	$(3\,1,-2)(2,2)$	$L10n_{85}$	$\{\{-1,1,1\},\{-1,-1,-1\},\{-1,-1,-1\},\{-1,1,-1\}\}$
17	$(2,2)(4,-2)$	$L10n_{86}$	$\{\{-1,-1,1\},\{-1,-1,-1\},\{1,-1,-1\},\{1,-1,1\}\}$
18	$4,3\,1,-2$	$L10n_{92}$	$\{\{-1,-1,1\},\{1,-1,-1\},\{-1,-1,-1\},\{1,-1,1\}\}$
19	$4,4,-2$	$L10n_{93}$	$\{\{-1,1,-1\},\{-1,-1,-1\},\{-1,1,1\},\{-1,1,-1\}\}$
20	$2\,0. - 2. - 2\,0.2\,0$	$L10n_{94}$	$\{\{-1,-1,1\},\{1,-1,-1\},\{1,-1,1\},\{1,-1,-1\}\}$
21	$3\,1,3\,1,-2$	$L10n_{95}$	$\{\{-1,-1,-1\},\{-1,-1,-1\},\{-1,1,-1\},\{-1,-1,-1\}\}$
22	$4\,1\,2\,2$	9_{11}	$\{\{-1,-1,-1\},\{-2,-1,-1\},\{-1,-1,-1\},\{-1,2,-1\}\}$
23	$4\,1\,1\,1\,2$	9_{14}	$\{\{-2,-1,-1\},\{-1,-2,-1\},\{-1,-1,-1\},\{-1,2,-1\}\}$
24	$2\,1\,3\,1\,2$	9_{17}	$\{\{-1,-1,-1\},\{-2,-1,-1\},\{-1,2,-1\},\{-1,-2,-1\}\}$
25	$2\,2\,1\,2\,2$	9_{23}	$\{\{-1,-1,-1\},\{-2,-2,-1\},\{-1,-1,-1\},\{-1,-1,-2\}\}$
26	$2\,1\,2\,1\,1\,2$	9_{27}	$\{\{-1,-1,-1\},\{-2,-1,-2\},\{-1,-1,-1\},\{-1,-2,-1\}\}$
27	$2\,1\,1\,1\,1\,1\,2$	9_{31}	$\{\{-2,-1,-1\},\{-1,-2,-1\},\{-1,-1,-1\},\{-2,-1,-1\}\}$
28	$6\,1\,2$	9^2_7	$\{\{-2,-1,-1\},\{-1,2,-1\},\{-1,-1,-1\},\{-1,2,-1\}\}$
29	$2\,2\,1\,1\,1\,2$	9^2_{12}	$\{\{-2,-1,-1\},\{-1,-1,-2\},\{-1,-1,-1\},\{-1,-2,-1\}\}$
30	$5,2,2$	9^2_{13}	$\{\{-1,-1,-1\},\{-2,2,-1\},\{-1,-1,-1\},\{-1,2,-1\}\}$
31	$.4$	9^2_{31}	$\{\{-2,-1,-1\},\{-1,2,-1\},\{-1,-1,-1\},\{-2,-1,-1\}\}$
32	$.3.2\,0$	9^2_{35}	$\{\{-2,-1,-1\},\{-1,-1,-2\},\{-1,-1,-1\},\{-1,2,-1\}\}$
33	8^*2	9^2_{42}	$\{\{-2,-1,-1\},\{-1,-1,-2\},\{-1,-1,-1\},\{-2,-1,-1\}\}$
34	$6\,2$	8_1	$\{\{-1,-1,-1\},\{-1,2,-1\},\{-1,2,-1\},\{-2,-2,-1\}\}$
35	$3,3,2$	8_5	$\{\{-1,-1,-1\},\{-2,-1,-1\},\{-1,2,-1\},\{-2,2,-1\}\}$
36	$4\,1\,1\,2$	8_7	$\{\{-2,-1,-1\},\{-2,-2,-1\},\{-1,-1,-1\},\{-1,2,-1\}\}$
37	$2\,3\,1\,2$	8_8	$\{\{-2,-1,-1\},\{-1,-1,-2\},\{-1,2,-1\},\{-1,-2,-1\}\}$
38	$2\,1,3,2$	8_{10}	$\{\{-2,-1,-1\},\{-1,-1,-2\},\{-2,-1,-1\},\{-1,2,-1\}\}$
39	$2\,2\,2\,2$	8_{12}	$\{\{-2,-1,-1\},\{-1,-2,-1\},\{-2,-1,-1\},\{-1,-2,-1\}\}$
40	$2\,2\,1\,1\,2$	8_{14}	$\{\{-2,-2,-1\},\{-1,-1,-2\},\{-1,-1,-1\},\{-2,-1,-1\}\}$
41	$.2.2\,0$	8_{16}	$\{\{-2,-1,-1\},\{-2,-2,-1\},\{-1,-1,-1\},\{-1,-1,-2\}\}$
42	$.2.2$	8_{17}	$\{\{-2,-1,-1\},\{-2,-1,-2\},\{-1,-1,-1\},\{-1,-1,-2\}\}$
43	8^*	8_{18}	$\{\{-2,-1,-1\},\{-2,-1,-1\},\{-1,-1,-1\},\{-2,-1,-1\}\}$
44	$2\,1\,2\,1\,2$	8^2_7	$\{\{-2,-1,2\},\{-1,-1,-2\},\{-1,-1,-1\},\{-2,-1,-1\}\}$
45	$2\,1\,1\,1\,1\,2$	8^2_8	$\{\{-2,-1,-1\},\{-2,-2,-1\},\{-1,-1,-1\},\{-2,-1,-1\}\}$
46	$4,2,2$	8^3_1	$\{\{-2,2,-1\},\{-1,-1,-2\},\{-1,-1,-1\},\{-1,2,-1\}\}$
47	$3\,1,2,2$	8^3_2	$\{\{-1,-1,1\},\{-1,-1,-1\},\{1,-1,-1\},\{-1,-1,-1\}\}$
48	$(2,2)(2,2)$	8^3_4	$\{\{-2,-1,-1\},\{-1,-1,-2\},\{-2,-1,-1\},\{-1,-1,-2\}\}$
49	$.3$	8^3_5	$\{\{-2,-1,-1\},\{-2,-1,-1\},\{-1,-1,-1\},\{-1,2,-1\}\}$
50	$.2 : 2\,0$	8^3_6	$\{\{-1,-1,-1\},\{-2,-1,-2\},\{-1,-1,-1\},\{-2,-1,-2\}\}$
51	$4,2,-2$	8^3_7	$\{\{-1,1,1\},\{1,-1,-1\},\{-1,1,-1\},\{1,-1,-1\}\}$
52	$3\,1,2,-2$	8^3_8	$\{\{-1,-1,1\},\{-1,-1,-1\},\{-1,1,-1\},\{-1,-1,-1\}\}$
53	$(2,2)(2,-2)$	8^3_9	$\{\{1,-1,1\},\{1,-1,-1\},\{1,-1,-1\},\{-1,-1,-1\}\}$
54	$(2,2) - (2,2)$	8^3_{10}	$\{\{-1,-1,-1\},\{-1,-1,-1\},\{-1,1,-1\},\{-1,1,-1\}\}$
55	$4\,3$	7_3	$\{\{-2,-1,-1\},\{-2,-2,-1\},\{-2,-1,-1\},\{-1,2,-1\}\}$
56	$3\,2\,2$	7_5	$\{\{-2,-2,-1\},\{-1,-1,-2\},\{-1,-1,-1\},\{-2,-1,-2\}\}$
57	$2,2,2+$	7^3_1	$\{\{-1,1,1\},\{-1,-1,-1\},\{1,1,-1\},\{-1,1,-1\}\}$
58	$2\,3\,2$	7^2_2	$\{\{-2,-2,-1\},\{-1,2,-2\},\{-1,-1,-1\},\{-2,-1,-1\}\}$
59	$3,2,2$	7^2_4	$\{\{-2,-1,-1\},\{-1,-1,-2\},\{-1,2,-1\},\{-2,2,-1\}\}$
60	$2\,1,2,2$	7^2_5	$\{\{-2,-1,-1\},\{-2,-1,-2\},\{-2,-1,-1\},\{-1,-1,-2\}\}$
61	$.2$	7^2_6	$\{\{-2,-1,-2\},\{-2,2,-1\},\{-1,-1,-1\},\{-1,-1,-2\}\}$
62	$2,2,2$	6^3_1	$\{\{-2,-1,-1\},\{-2,-1,-2\},\{-2,-1,-1\},\{-2,-1,-2\}\}$
63	6^*	6^3_2	$\{\{-2,-1,-1\},\{-2,-1,-2\},\{-1,-1,-1\},\{-2,2,-2\}\}$
64	$2,2,-2$	6^3_3	$\{\{-1,-1,1\},\{-1,1,-1\},\{1,-1,-1\},\{-1,-1,-1\}\}$

Table 3: *KL*s derived from *RG*[3, 3]

21
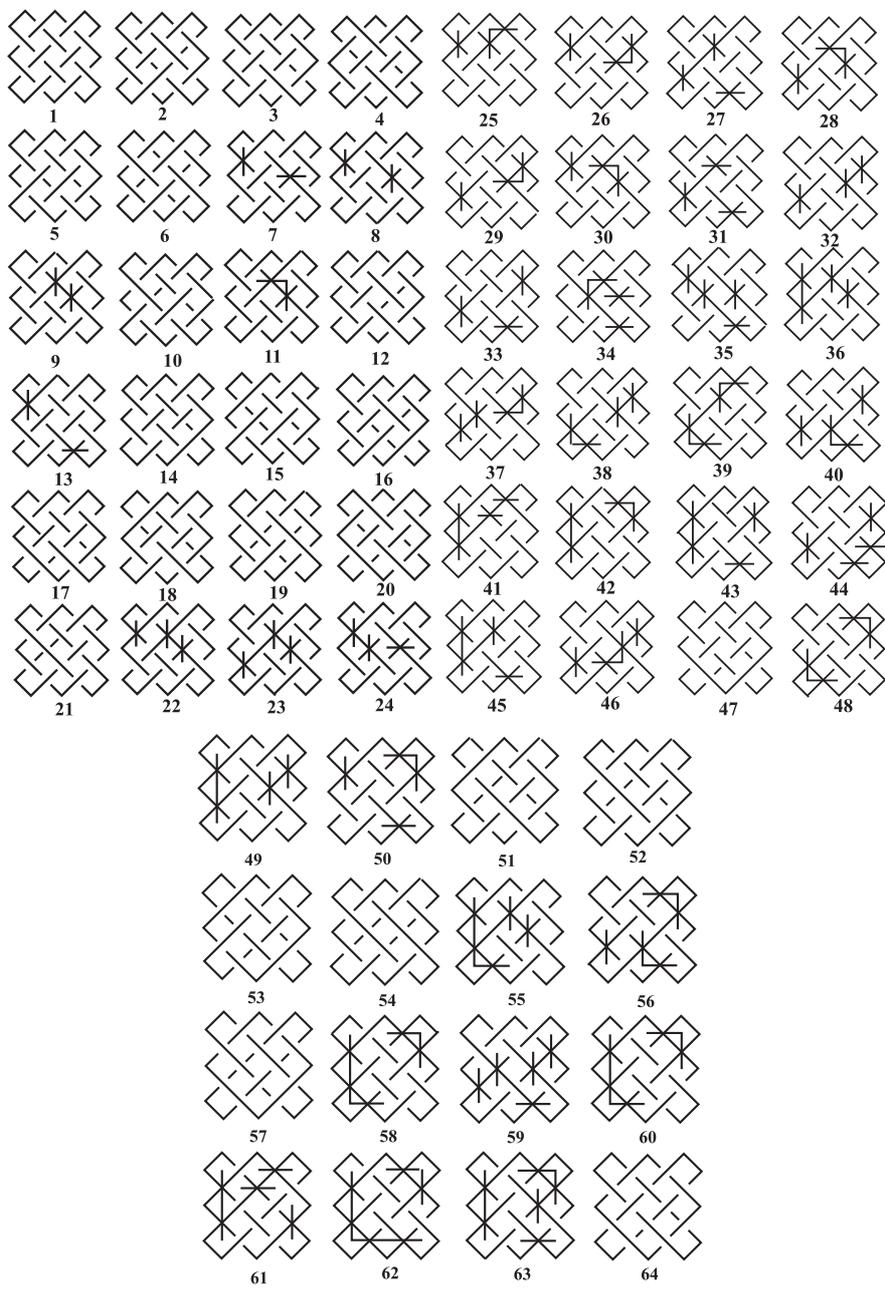
Figure 23: Mirror-curves 1-64 derived from $RG[3, 3]$.